GUIDED WAVES IN SLIGHT, AZIMUTHALLY ANISOTROPIC FORMATIONS

by

K. J. Ellefsen and C. H. Cheng

Earth Resources Laboratory
Department of Earth, Atmospheric, and Planetary Sciences
Massachusetts Institute of Technology
Cambridge, MA 02139

ABSTRACT

A method of calculating dispersion curves for guided waves in slight, azimuthally anisotropic formations is developed with perturbation theory. The fluid is assumed to be inviscid, the formation perfectly elastic and homogeneous, and the borehole wall cylindrical. The first step is calculating the elastic moduli for a transversely isotropic formation whose moduli are close to those for the azimuthally anisotropic formation. The perturbative method then uses the particle displacements for a guided wave in the transversely isotropic formation and the difference between the elastic moduli in the two formations to determine a first order correction to the wavenumber. These corrections are used to calculate the perturbation in the phase velocity. To test the method, the elastic moduli of an isotropic formation were perturbed to make it transversely isotropic. The exact dispersion curves and those estimated by the perturbative method are very close. The perturbative method was used to calculate dispersion curves for guided waves in two different geologic settings — a formation with aligned, vertical cracks and another with a tilted bed. In both examples the dispersion curves for the guided waves appear similar to typical dispersion curves for either isotropic or transversely isotropic formations. At low frequencies, the phase velocities of the tube waves closely match the velocities predicted by Rice's formula.

INTRODUCTION

Knowledge of azimuthal velocity anisotropy is important in the earth sciences and particularly in hydrocarbon exploration and production. (Here azimuthal anisotropy is defined to be a characteristic of a formation in which the seismic velocity changes with azimuth.) Because this anisotropy is sometimes caused by aligned fractures, it might be used to predict the direction of fluid flow in a reservoir and to estimate the horizontal components of stress. Two S-waves with different polarizations exist

in azimuthally anisotropic formations, and these directions must be known for proper processing and interpretation of S-wave, surface seismic data.

Acoustic logging might be used to detect azimuthal anisotropy. The shear moduli are the most important properties of isotropic and transversely isotropic formations in determining the velocity dispersion of the guided waves (Cheng et al., 1982; Ellefsen et al., 1988). (Here transverse isotropy is defined to be a characteristic of a formation in which the seismic velocity is constant with azimuth. That is, the formation is anisotropic with hexagonal symmetry, and the symmetry axis is parallel to the borehole.) A reasonable supposition is that the elastic moduli related to S-wave propagation in an azimuthally anisotropic formation might also be important in determining the dispersion of the guided waves. However, little has been published on this topic. Rice (1987) presented a method of estimating the S-wave anisotropy using the velocities of the screw wave at its cutoff frequency and of the tube wave at very low frequencies, but he did not state how anisotropy affects a guided wave in the frequency range normally used in acoustic logging.

The purpose of this paper is to show how dispersion curves can be calculated for guided waves in slight, azimuthally anisotropic formations. To this end, we will use a method based upon perturbation theory and Hamilton's variational principle, which is an extension of a method that we previously used to study guided waves in transversely isotropic formations (Ellefsen and Cheng, 1988). Smith and Dahlen (1973) used the same approach to estimate the effect of slight anisotropy in the Earth's crust upon the phase velocity of surface waves. Dispersion curves will be calculated for tube, pseudo-Rayleigh, flexural, and screw waves in two hypothetical formations — one with aligned, vertical cracks and another with a tilted bed.

METHOD

Analytical solutions for the velocity of guided waves in azimuthally anisotropic formations are difficult to obtain because the tensor of elastic moduli and hence the displacements and tractions vary with azimuth. Therefore, a perturbative method might be a reasonable approach to obtain a solution for guided waves in slightly anisotropic formations. With this method, the starting point must be a guided wave in either an isotropic formation or transversely isotropic formation which are the only two cases for which analytical solutions currently exist. Furthermore, the fluid is assumed to be inviscid, the formation perfectly elastic and homogeneous, and the borehole wall cylindrical. At each frequency, the wave can be described by its wavenumber and particle displacements. A slight change in the elastic properties of the formation will cause a slight change in the wavenumber and the displacements. (Alternatively, at each wavenumber, a change in the elastic properties would alter the frequency and displacements. Because current signal processing methods calculate wavenumber at

constant frequency, we will study the former case.) Hamilton's variational principle shows that the changes in the displacements of normal modes (e.g., tube and pseudo-Rayleigh waves) have, to first order, no effect upon the Lagrangian energy and hence can be neglected. The perturbation in the elastic properties of the formation can then be directly related to the perturbation in the wavenumber, which is expressed by this equation:

$$\int_t^{t+\mathcal{T}} dt \int_V dV \delta_W e_{ij} \hat{c}_{ijkl} e_{kl} = -\frac{1}{2} \int_t^{t+\mathcal{T}} dt \int_V dV e_{ij} \delta c_{ijkl} e_{kl} \qquad (1)$$

(Ellefsen and Cheng, 1989). The original elastic properties of the fluid and formation are represented by the tensor, $\hat{c}_{ijkl}$, and the strain by e_{ij}. The perturbation in the elastic moduli of the formation is shown explicitly by δc_{ijkl}, and the perturbation in the wavenumber implicitly by $\delta_W e_{ij}$. The volume integral applies to a disk having the thickness of one wavelength and extending to infinity away from the axis of the borehole. The integral is finite because the strains are everywhere finite and are zero at infinity. The time integral extends over one period, $\mathcal{T}$.

Calculating dispersion curves for guided waves propagating along a borehole through a slightly anisotropic formation requires four steps. First, the elastic moduli for a transversely isotropic formation which is close to the slightly anisotropic formation must be calculated. "Closeness", which will be defined later, is important because it maximizes the range in which the perturbative solution is accurate. Because a transversely isotropic formation has more elastic moduli than an isotropic formation, it can be closer to the azimuthally anisotropic formation, and hence it is always used as the starting point. Second, the phase velocity and wavenumber for the guided wave in the transversely isotropic formation are determined at each frequency. The particle displacements for this guided wave in the transversely isotropic formation must be similar to those for the guided wave in the azimuthally anisotropic formation. Third, the perturbation in the wavenumber, δl, due to the perturbations in the elastic moduli is calculated at each frequency using equation 1. The perturbation in the phase velocity can be directly calculated with

$$\delta v = -v \delta l / l \quad . \qquad (2)$$

Fourth, this correction is added to the original dispersion curve for the transversely isotropic formation.

An optimization technique, which is based upon a method developed by Backus (1982) for isotropic formations, is used to make the transversely isotropic formation close to the azimuthally anisotropic formation. The elastic tensor for the anisotropic medium is written as a sum of its transversely isotropic and aelotropic parts: $c_{ijkl} = \hat{c}_{ijkl} + \delta c_{ijkl}$. In geometric terms, $\hat{c}_{ijkl}$ is the orthogonal projection of c_{ijkl} onto the space which contains all transversely isotropic tensors. The aelotropic tensor, δc_{ijkl}, is defined as the orthogonal complement to that space. To make the best approximation, the most amount of c_{ijkl} must be put into $\hat{c}_{ijkl}$, and the least amount into δc_{ijkl}.

Pythagoras' theorem, $||c_{ijkl}||^2 = ||\hat{c}_{ijkl}||^2 + ||\delta c_{ijkl}||^2$, shows that this situation occurs when $||\delta c_{ijkl}||^2$ is minimized. A qualitative measure of the amount of the anisotropy is the relative size of the aelotropic tensor, $||\delta c_{ijkl}||^2 / ||\hat{c}_{ijkl}||^2$, and will be called the anisotropic strength.

Equation 1 is evaluated using the expressions for the displacements listed in Appendix A. The first integral is

$$\int_t^{t+\mathcal{T}} dt \int_V dV \delta_W e_{ij} \hat{c}_{ijkl} e_{kl} = \delta l \frac{\zeta \pi \Lambda \mathcal{T}}{4} I^l \quad . \tag{3}$$

The integration over time yields $\mathcal{T}/2$. The volume integral is computed in the circular cylindrical coordinate system with coordinates r, θ, and z. The integration over z yields $\Lambda/2$, and over azimuth $\zeta\pi$. When the azimuthal order number is 0, $\zeta = 2$; otherwise $\zeta = 1$. The integration over radius, which cannot be computed analytically, is simply given the generic designation I and is listed in Appendix B. When the second integral in equation 1 is evaluated, the aelotropic tensor must be computed for every azimuth. Using abbreviated subscript notation, this transformation is performed with

$$[\delta c'] = [M][\delta c][M]^T \quad , \tag{4}$$

in which $[\delta c]$ is the aelotropic matrix at $\theta = 0$, $[\delta c']$ the aelotropic matrix at angle θ, and

$$[M] = \begin{bmatrix} \cos^2\theta & \sin^2\theta & 0 & 0 & 0 & \sin 2\theta \\ \sin^2\theta & \cos^2\theta & 0 & 0 & 0 & -\sin 2\theta \\ 0 & 0 & 1 & 0 & 0 & 0 \\ 0 & 0 & 0 & \cos\theta & -\sin\theta & 0 \\ 0 & 0 & 0 & \sin\theta & -\cos\theta & 0 \\ -\frac{1}{2}\sin 2\theta & \frac{1}{2}\sin 2\theta & 0 & 0 & 0 & \cos 2\theta \end{bmatrix} \tag{5}$$

(Auld, 1973). (This transformation is not applied to $\hat{c}_{ijkl}$ because it is the same at all azimuths.) The integral for the perturbations in the elastic moduli is

$$\int_t^{t+\mathcal{T}} dt \int_V dV e_{ij} \delta c_{ijkl} e_{kl} = \frac{\zeta \pi \Lambda \mathcal{T}}{4} \sum_{i=1}^{21} \delta c_i I^{c_i} \tag{6}$$

in which δc_i is the perturbation in one of the 21 moduli. The integral over radius, I^{c_i}, is listed in Appendix B for azimuthal order numbers 0, 1, and 2. Combining equations 2, 3, and 6 gives the perturbation in the phase velocity due to the perturbations in the moduli:

$$\delta v = \frac{\omega}{2l^2} \frac{\sum_{i=1}^{21} \delta c_i I^{c_i}}{I^l} \quad . \tag{7}$$

RESULTS AND DISCUSSION

Test results show that the phase velocities obtained by this perturbative method are quite accurate. Exact dispersion curves were calculated for a transversely isotropic formation, which was selected to be Mesaverde shale (3883) whose physical properties are listed by Thomsen (1986). The isotropic part of the transversely isotropic tensor was determined using Backus' (1982) technique. (For this test case, $\hat{c}_{ijkl}$ are the moduli for the isotropic formation, and δc_{ijkl} are the perturbations which make the isotropic formation transversely isotropic.) The anisotropic strength is 0.10. After calculating the dispersion curves for the isotropic formation, velocity corrections which were computed with the perturbative method were added to account for the transverse isotropy. Figure 1 shows that the estimated velocities for the tube wave are very close to the exact solution, and similar results were obtained for the other guided waves.

Dispersion curves were calculated for guided waves in two different geological settings in which the formation is azimuthally anisotropic. The first formation contains aligned, vertical cracks (Figure 2a). Because the cracks are small compared to the wavelengths which are studied here, this heterogeneous medium can be modeled as being homogeneous and anisotropic. The anisotropy has hexagonal symmetry with a horizontal symmetry axis, which is perpendicular to the cracks and also the borehole axis. The elastic moduli are the same as those for the Mesaverde limestone (5496.5) and are listed by Thomsen (1986). The anisotropic strength is 0.034. The polarization directions for vertically propagating, planar S-waves are parallel and perpendicular to the cracks, and phase velocities were calculated for guided waves oriented in the same directions (Figure 2b). The velocities for the tube, pseudo-Rayleigh, and screw waves are the same for both orientations, whereas those for the flexural wave are not. The phase velocity for the flexural wave oriented parallel to the cracks is always higher, and the difference increases from high to low frequencies.

The second formation represents either a tilted bed perforated by a vertical borehole or a horizontal bed perforated by a deviated borehole (Figure 3a). The anisotropy has hexagonal symmetry with a symmetry axis tilted ten degrees with respect to the borehole axis. The rock's physical properties match those of the Taylor sandstone which are tabulated by Thomsen (1986), and the anisotropic strength is 0.023. The polarization directions of vertically propagating, planar S-waves is along the strike and dip directions, and dispersion curves were calculated for guided waves oriented in the same directions (Figure 3b). Like the previous example, the phase velocities of the tube, pseudo-Rayleigh, and screw waves are the same for both orientations, but those for the flexural wave differ. In both examples, the dispersion curves for the tube, pseudo-Rayleigh, and screw waves appear similar to curves for related guided waves in either isotropic or transversely isotropic formations.

At low frequencies the phase velocities of the tube waves closely match the values

Model	Tube Wave Velocity (km/s)	
	Rice's Formula	Perturbative Method
vertical cracks	1.4290	1.4319
tilted bed	1.3806	1.3808

Table 1: Comparison of velocities predicted by Rice's formula and the perturbative method.

predicted by Rice's formula (1987). Rice studied an anisotropic formation with hexagonal symmetry in which the symmetry axis was tilted at angle, ψ, with respect to the borehole axis. He found that as the frequency approaches zero, the phase velocity of the tube wave approaches

$$v = \sqrt{\frac{(c_{66}\cos^2\psi + c_{44}\sin^2\psi)v_f}{(c_{66}\cos^2\psi + c_{44}\sin^2\psi) + \rho_f v_f^2}} \quad . \tag{8}$$

The fluid density and acoustic velocity are ρ_f and v_f, and the shear elastic moduli for the formation are c_{44} and c_{66}. Using this formula, the velocity of the tube wave at 0 Hz was calculated for both geologic situations and was compared to the velocity predicted by the perturbative method at 1 Hz (Table 1). For the vertical crack model the difference between the velocities is 0.0029 km/s, and for the tilted bed model 0.0002 km/s.

To properly apply the perturbative method, the particle displacements and the elastic moduli for the guided wave in the transversely isotropic formation must be close to those for the guided wave in the azimuthally anisotropic formation. Picking the best elastic moduli for the transversely isotropic formation was done with the optimization technique. However, no straightforward method exists for picking the best displacements. We believe that the displacements for the guided waves in the transversely isotropic formation are adequate except, perhaps, when the phase velocity is close to the S-wave velocity. That is, in the transversely isotropic formations the phase velocities of the pseudo-Rayleigh and screw waves at their cutoff frequencies and of the flexural wave at low frequencies equal the vertical S-wave velocity. Because two vertically propagating S-waves exist in anisotropic formations, the particle displacements of the guided wave, when its velocity is close to one of the S-wave velocities, might differ significantly from the displacements for the related guided wave in the transversely isotropic formation. For this reason, we question the accuracy of the dispersion curves near the S-wave velocities and are doing additional work to resolve this issue.

CONCLUSIONS

A perturbative method for calculating the velocity dispersion of guided waves in slight, azimuthally anisotropic formations was developed. To implement this method, four steps are required: (1) elastic moduli for a transversely isotropic formation, which are close to those for the azimuthally anisotropic formation, are picked with an optimization technique, (2) the phase velocity and wavenumber of the guided waves in the transversely isotropic formation are calculated at each frequency, (3) equation 1 is used to calculate the perturbation in wavenumber and velocity due to the change in elastic moduli between the two formations, and (4) the velocity perturbation is added to the original dispersion curve. An important assumption is that the displacements for the wave in the transversely isotropic formations are similar to those in the azimuthally anisotropic formation.

The accuracy of the perturbative method was demonstrated in two ways. First, the elastic moduli for an isotropic formation were perturbed to make it transversely isotropic. The phase velocities calculated with the perturbative method were very close to the exact velocities at all frequencies. Second, Rice's formula was used to predict the phase velocities at 0 Hz of the tube waves in the anisotropic formations. The velocities from this formula and the velocities calculated by the perturbative method for a wave at 1 Hz are close.

The perturbative method was used to calculate the velocity dispersion of guided waves in two different geologic settings — a formation with aligned, vertical cracks and another with a tilted bed. Velocities were calculated for waves oriented along the polarization directions of the two vertically propagating S-waves. In both formations, the waves behave similarly. The tube, pseudo-Rayleigh, and screw waves have the same dispersion curves for both orientations, but the flexural wave does not. The velocity of the flexural wave, oriented parallel to the polarization of the fastest S-wave, is always higher than the velocity of the wave oriented parallel to the polarization of the slowest S-wave. The velocities of the guided waves near the S-wave velocities may be inaccurate, and when this problem is resolved, we should be able to determine whether acoustic logging can detect azimuthal anisotropy.

ACKNOWLEDGEMENTS

This work was supported by the Full Waveform Acoustic Logging Consortium at MIT. K. J. Ellefsen is partially supported by the Phillips Petroleum Fellowship.

REFERENCES

Auld, B. A., *Acoustic Fields and Waves in Solids,* vol. 1, John Wiley & Sons, Inc., 1973.

Backus, G. E., Reply: Limits of validity of first-order perturbation theory of quasi-P velocity in weakly anisotropic media, *J. Geophys. Res., 87,* 4641–4644, 1982.

Cheng, C. H., M. N. Toksöz, and M. E. Willis, Determination of in situ attenuation from full waveform acoustic logs, *J. Geophys. Res., 87,* 5477–5484, 1982.

Ellefsen, K. J. and C. H. Cheng, Applications of perturbation theory to acoustic logging, this report.

Ellefsen, K. J., C. H. Cheng, and D. P. Schmitt, Acoustic logging guided waves in transversely isotropic formations, in *Trans. SPWLA 29th Ann. Logging Symp.,* 1988, paper YY.

Rice, J. A., A method for logging shear wave velocity anisotropy, in *57th Ann. Internat. Mtg., Soc. Explor. Geophys., Expd. Abst.,* 27–28, New Orleans, LA, 1987.

Smith, M. L. and F. A. Dahlen, The azimuthal dependence of Love and Rayleigh wave propagation in a slightly anisotropic medium, *J. Geophys. Res., 78,* 3321–3333, 1973.

Thomsen, L., Weak elastic anisotropy, *Geophysics, 51,* 1954–1966, 1986.

Tongtaow, C., *Wave propagation along a cylindrical borehole in a transversely isotropic formation,* Ph.D. thesis, Colorado School of Mines, 1982.

APPENDIX A

The equations for the displacements and strains associated with a normal mode in a fluid-filled borehole are presented in this appendix. These equations are based upon the expressions which Tongtaow (1982) derived for a travelling wave in a borehole with a tool.

The displacements have this general form:

$$\begin{aligned} u_r(r,\theta,z,t) &= \frac{1}{2}\left[U_r(r)e^{ilz} + U_r^*(r)e^{-ilz}\right]\cos(n\theta)\cos(\omega t) \\ u_\theta(r,\theta,z,t) &= \frac{1}{2}\left[U_\theta(r)e^{ilz} + U_\theta^*(r)e^{-ilz}\right]\sin(n\theta)\cos(\omega t) \\ u_z(r,\theta,z,t) &= \frac{1}{2}\left[U_z(r)e^{ilz} + U_z^*(r)e^{-ilz}\right]\cos(n\theta)\cos(\omega t) \quad . \end{aligned} \tag{A-1}$$

In the circular cylindrical coordinate system, r is the radial distance, z the axial distance, and θ the azimuth. The axial wavenumber is l, the azimuthal order number n, and the radian frequency ω. The functions for the radial dependence of the displacements in the fluid are

$$\begin{aligned} U_r(r) &= A_1 m_1\left[\frac{n}{m_1 r}I_n(m_1 r) + I_{n+1}(m_1 r)\right] \\ U_\theta(r) &= -\frac{A_1 n}{r}I_n(m_1 r) \\ U_z(r) &= A_1 il I_n(m_1 r) \quad , \end{aligned} \tag{A-2}$$

and in the formation are

$$\begin{aligned} U_r(r) &= -A_2 m_2(1+ila')\left[-\frac{n}{m_2 r}K_n(m_2 r) + K_{n+1}(m_2 r)\right] + \\ &\quad \frac{C_2 n}{r}K_n(\bar{k}_2 r) - B_2 k_2(il+b')\left[-\frac{n}{k_2 r}K_n(k_2 r) + K_{n+1}(k_2 r)\right] \\ U_\theta(r) &= -\frac{A_2 n}{r}(1+ila')K_n(m_2 r) + C_2\bar{k}_2\left[-\frac{n}{\bar{k}_2 r}K_n(\bar{k}_2 r) + K_{n+1}(\bar{k}_2 r)\right] - \\ &\quad \frac{B_2 n}{r}(il+b')K_n(k_2 r) \\ U_z(r) &= A_2(il - a'm_2^2)K_n(m_2 r) - B_2(k_2^2 - ilb')K_n(k_2 r) \end{aligned} \tag{A-3}$$

The coefficients, A_1, A_2, B_2, and C_2, and the axial wavenumber are found by solving the period equation. Formulas for the wavenumbers, m_1, m_2, k_2, and $\bar{k}_2$, and the coupling coefficients, a' and b', are given by Tongtaow (1982).

APPENDIX B

Expressions for the integrals in equation 1, appropriate for a fluid-filled borehole through a transversely isotropic formation, are presented in this appendix.

The strains are found by differentiating the displacements listed in Appendix A, and the radial parts are designated E_{rr}, $E_{\theta\theta}$, E_{zz}, $E_{z\theta}$, E_{rz}, and $E_{r\theta}$. The displacements and strains are substituted into the integrals in equation 1, and almost all of the integrals are computed analytically. In the final expressions for the integrals ζ is 2 when $n = 0$; otherwise ζ is 1. When $n = 0$, all displacements and strains containing $\sin(n\theta)$ cancel. Because the radial dependence of these particular displacements and strains are also zero when $n = 0$, they may be included in the integrals eliminating the need to write the equations twice.

The integral associated with a perturbation in wavenumber is

$$\int_t^{t+\mathcal{T}} dt \int_V dV \delta_W e_{ji} c_{ijkl} e_{lk} = \delta l \frac{\zeta \pi \Lambda \mathcal{T}}{4} \times \tag{B-1}$$

$$\left(\int_0^R dr\, r \lambda_f \Big[|E_{rr}||iU_z| \cos\left(\arg E_{rr} - \arg(iU_z)\right) + \right.$$

$$|E_{\theta\theta}||iU_z| \cos\left(\arg E_{\theta\theta} - \arg(iU_z)\right) + |E_{zz}||iU_z| \cos\left(\arg E_{zz} - \arg(iU_z)\right) \Big] +$$

$$\int_R^\infty dr\, r \Big\{ c_{13} \Big[|E_{rr}||iU_z| \cos\left(\arg E_{rr} - \arg(iU_z)\right) +$$

$$|E_{\theta\theta}||iU_z| \cos\left(\arg E_{\theta\theta} - \arg(iU_z)\right) \Big] + c_{33} \Big[|E_{zz}||iU_z| \cos\left(\arg E_{zz} - \arg(iU_z)\right) \Big] +$$

$$c_{44} \Big[4|E_{z\theta}| \Big| \frac{iU_\theta}{2} \Big| \cos(\arg E_{z\theta} - \arg(\frac{iU_\theta}{2})) +$$

$$\left. 4|E_{rz}| \Big| \frac{iU_r}{2} \Big| \cos(\arg E_{rz} - \arg(\frac{iU_r}{2})) \Big] \Big\} \right) \quad ,$$

in which R is the borehole radius. The sum of the two integrals over radius will be designated I^l.

The integral associated with the perturbed elastic moduli is

$$\int_t^{t+\mathcal{T}} dt \int_V dV e_{ji} \delta c_{ijkl} e_{lk} = \frac{\zeta \pi \Lambda \mathcal{T}}{4} \times$$

$$\int_R^\infty dr\, r \Big\{ d_{11}|E_{rr}|^2 + d_{12} 2|E_{rr}||E_{\theta\theta}| \cos(\arg E_{rr} - \arg E_{\theta\theta}) +$$

$$d_{13} 2|E_{rr}||E_{zz}| \cos(\arg E_{rr} - \arg E_{zz}) + d_{16} 4|E_{rr}||E_{r\theta}| \cos(\arg E_{rr} - \arg E_{r\theta}) +$$

$$d_{22}|E_{\theta\theta}|^2 + d_{23} 2|E_{\theta\theta}||E_{zz}| \cos(\arg E_{\theta\theta} - \arg E_{zz}) +$$

$$d_{26} 4|E_{\theta\theta}||E_{r\theta}| \cos(\arg E_{\theta\theta} - \arg E_{r\theta}) +$$

$$d_{33}|E_{zz}|^2 + d_{36} 4|E_{zz}||E_{r\theta}| \cos(\arg E_{zz} - \arg E_{r\theta}) +$$

$$d_{44}4|E_{z\theta}|^2 + d_{45}8|E_{z\theta}||E_{rz}|\cos(\arg E_{z\theta} - \arg E_{rz}) +$$
$$d_{55}4|E_{rz}|^2 + d_{66}4|E_{r\theta}|^2\Big\} \quad . \tag{B-2}$$

for which the integral over radius will be designated $\sum_{i=1}^{21} \delta c_i I^{c_i}$. When $n = 0$,

$$\begin{aligned}
d_{11} &= \frac{1}{2}\delta c_{66} + \frac{3}{8}\delta c_{22} + \frac{1}{4}\delta c_{12} + \frac{3}{8}\delta c_{11} \\
d_{12} &= -\frac{1}{2}\delta c_{66} + \frac{1}{8}\delta c_{22} + \frac{3}{4}\delta c_{12} + \frac{1}{8}\delta c_{11} \\
d_{13} &= \frac{1}{2}\delta c_{23} + \frac{1}{2}\delta c_{13} \\
d_{16} &= 0 \\
d_{22} &= \frac{1}{2}\delta c_{66} + \frac{3}{8}\delta c_{22} + \frac{1}{4}\delta c_{12} + \frac{3}{8}\delta c_{11} \\
d_{23} &= \frac{1}{2}\delta c_{23} + \frac{1}{2}\delta c_{13} \\
d_{26} &= 0 \\
d_{33} &= \delta c_{33} \\
d_{36} &= 0 \\
d_{44} &= 0 \\
d_{45} &= 0 \\
d_{55} &= \frac{1}{2}\delta c_{55} + \frac{1}{2}\delta c_{44} \\
d_{66} &= 0 \quad ,
\end{aligned} \tag{B-3}$$

and when $n = 1$,

$$\begin{aligned}
d_{11} &= \frac{1}{2}\delta c_{66} + \frac{1}{8}\delta c_{22} + \frac{1}{4}\delta c_{12} + \frac{5}{8}\delta c_{11} \\
d_{12} &= -\frac{1}{2}\delta c_{66} + \frac{1}{8}\delta c_{22} + \frac{3}{4}\delta c_{12} + \frac{1}{8}\delta c_{11} \\
d_{13} &= \frac{1}{4}\delta c_{23} + \frac{3}{4}\delta c_{13} \\
d_{16} &= \frac{1}{8}\delta c_{22} - \frac{1}{8}\delta c_{11} \\
d_{22} &= \frac{1}{2}\delta c_{66} + \frac{5}{8}\delta c_{22} + \frac{1}{4}\delta c_{12} + \frac{1}{8}\delta c_{11} \\
d_{23} &= \frac{3}{4}\delta c_{23} + \frac{1}{4}\delta c_{13} \\
d_{26} &= \frac{1}{8}\delta c_{22} - \frac{1}{8}\delta c_{11} \\
d_{33} &= \delta c_{33} \\
d_{36} &= \frac{1}{4}\delta c_{23} - \frac{1}{4}\delta c_{13}
\end{aligned}$$

$$
\begin{aligned}
d_{44} &= \frac{3}{4}\delta c_{55} + \frac{1}{4}\delta c_{44} \\
d_{45} &= \frac{1}{4}\delta c_{44} - \frac{1}{4}\delta c_{55} \\
d_{55} &= \frac{3}{4}\delta c_{55} + \frac{1}{4}\delta c_{44} \\
d_{66} &= \frac{1}{2}\delta c_{66} + \frac{1}{8}\delta c_{22} - \frac{1}{4}\delta c_{12} + \frac{1}{8}\delta c_{11} \quad , \qquad \text{(B-4)}
\end{aligned}
$$

and when $n = 2$,

$$
\begin{aligned}
d_{11} &= \frac{1}{4}\delta c_{66} + \frac{7}{16}\delta c_{22} + \frac{1}{8}\delta c_{12} + \frac{7}{16}\delta c_{11} \\
d_{12} &= -\frac{1}{4}\delta c_{66} + \frac{1}{16}\delta c_{22} + \frac{7}{8}\delta c_{12} + \frac{1}{16}\delta c_{11} \\
d_{13} &= \frac{1}{2}\delta c_{23} + \frac{1}{2}\delta c_{13} \\
d_{16} &= \frac{1}{4}\delta c_{66} - \frac{1}{16}\delta c_{22} + \frac{1}{8}\delta c_{12} - \frac{1}{16}\delta c_{11} \\
d_{22} &= \frac{1}{4}\delta c_{66} + \frac{7}{16}\delta c_{22} + \frac{1}{8}\delta c_{12} + \frac{7}{16}\delta c_{11} \\
d_{23} &= \frac{1}{2}\delta c_{23} + \frac{1}{2}\delta c_{13} \\
d_{26} &= -\frac{1}{4}\delta c_{66} + \frac{1}{16}\delta c_{22} - \frac{1}{8}\delta c_{12} + \frac{1}{16}\delta c_{11} \\
d_{33} &= \delta c_{33} \\
d_{36} &= 0 \\
d_{44} &= \frac{1}{2}\delta c_{55} + \frac{1}{2}\delta c_{44} \\
d_{45} &= 0 \\
d_{55} &= \frac{1}{2}\delta c_{55} + \frac{1}{2}\delta c_{44} \\
d_{66} &= \frac{1}{4}\delta c_{66} + \frac{3}{16}\delta c_{22} - \frac{3}{8}\delta c_{12} + \frac{3}{16}\delta c_{11} \quad . \qquad \text{(B-5)}
\end{aligned}
$$

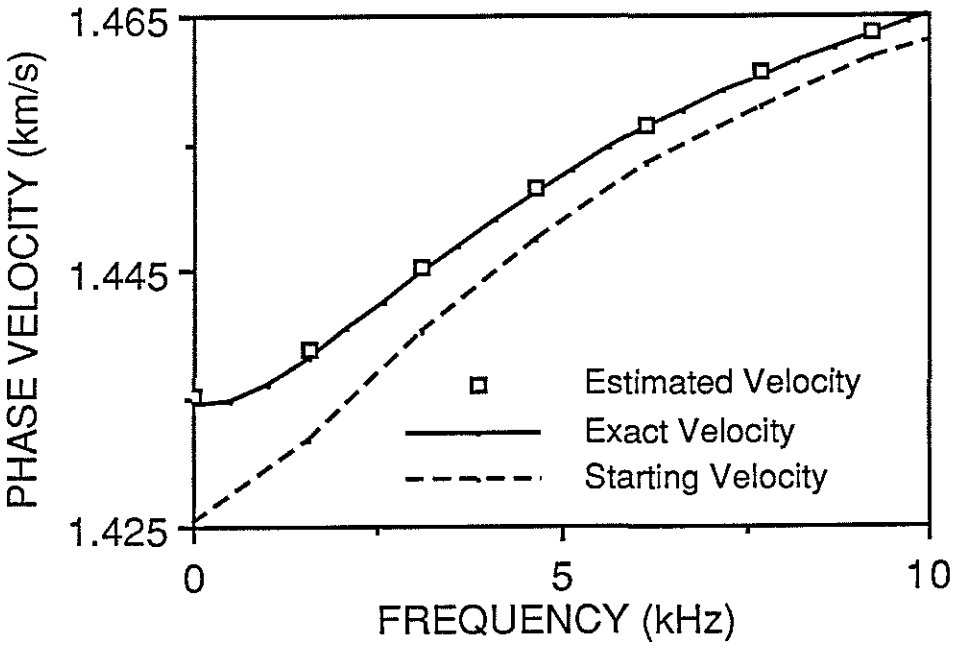

Figure 1: Accuracy of the phase velocity of a tube wave estimated by the perturbative method. The starting model was an isotropic formation and the perturbative method estimated the velocities for a transversely isotropic formation.

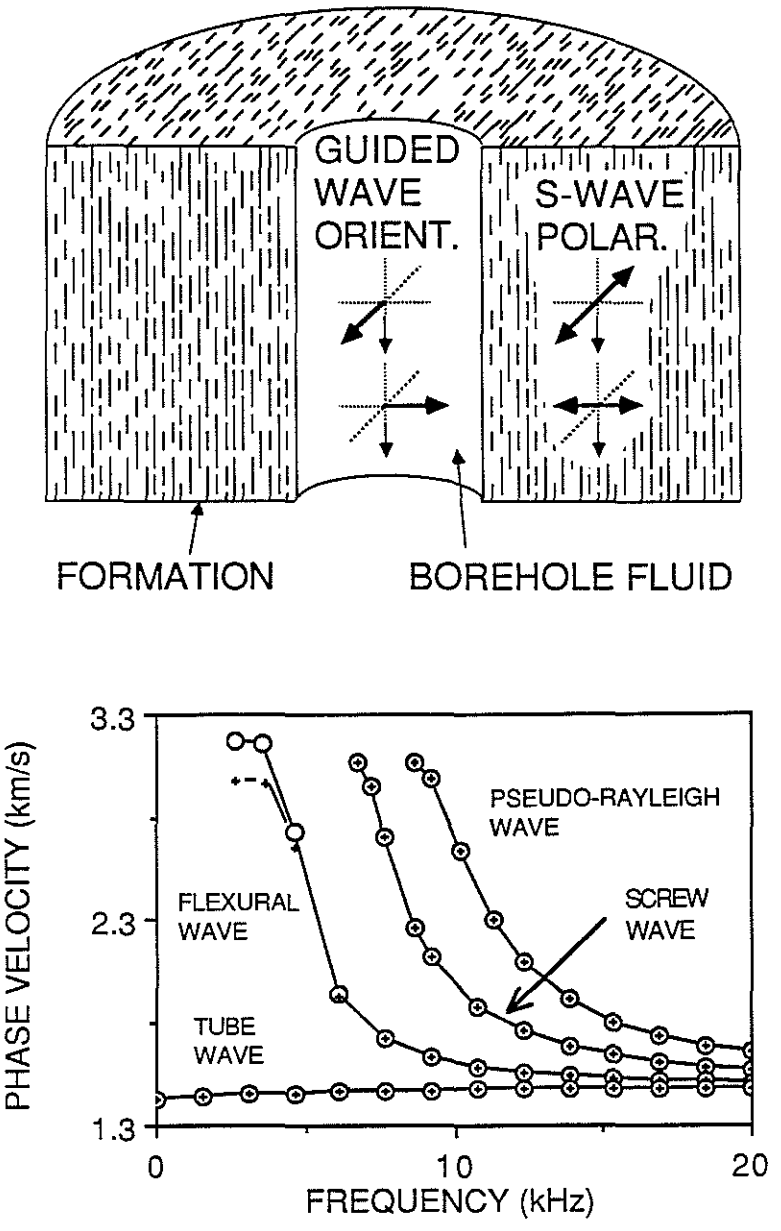

Figure 2: (a) Borehole through a hypothetical formation which has aligned, vertical cracks and is modeled as an azimuthally anisotropic formation. (b) Phase velocities for guided waves oriented parallel (circles) and perpendicular (plus signs) to the cracks.

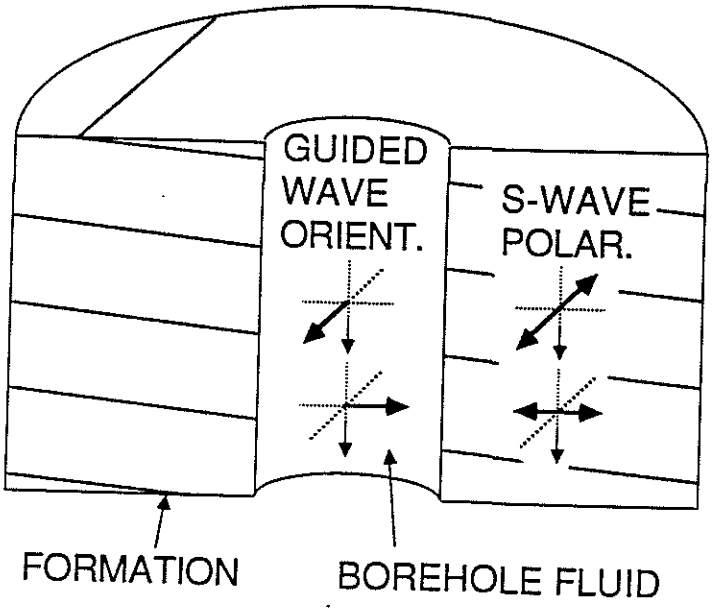

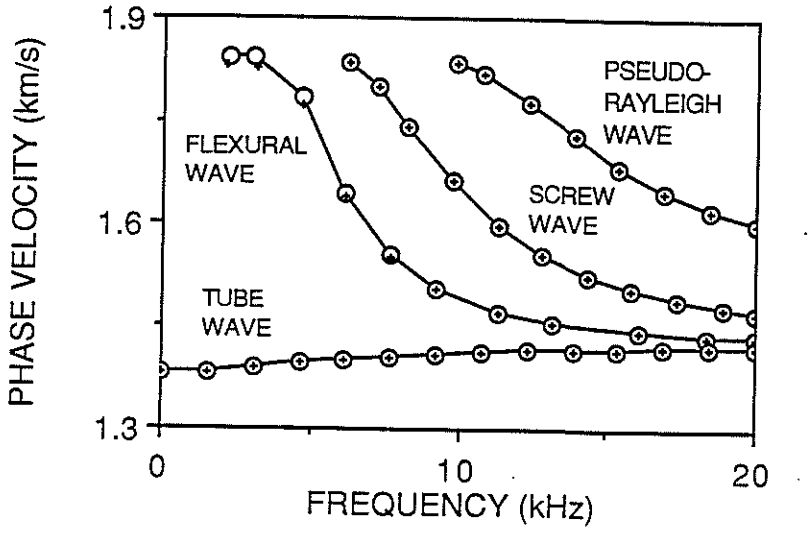

Figure 3: (a) Borehole through a hypothetical formation which has a tilted bed and is modeled as an azimuthally anisotropic formation. (b) Phase velocities for guided waves oriented along the strike (circles) and dip (plus signs).